

BEURLING-SELBERG EXTREMIZATION FOR DUAL-BLIND DECONVOLUTION RECOVERY IN JOINT RADAR-COMMUNICATIONS

Jonathan Monsalve*, Edwin Vargas[†], Kumar Vijay Mishra[‡], Brian M. Sadler[‡] and Henry Arguello[†]

[†]Universidad Industrial de Santander, Bucaramanga, Colombia, 680002

*Corporación Universitaria Minuto de Dios, Bogotá, Colombia, 111021

[‡]United States DEVCOM Army Research Laboratory, Adelphi, MD 20783 USA

ABSTRACT

Recent interest in integrated sensing and communications has led to the design of novel signal processing techniques to recover information from an overlaid radar-communications signal. Here, we focus on a spectral coexistence scenario, wherein the channels and transmit signals of both radar and communications systems are unknown to the common receiver. In this dual-blind deconvolution (DBD) problem, the receiver admits a multi-carrier wireless communications signal that is overlaid with the radar signal reflected off multiple targets. The communications and radar channels are represented by continuous-valued range-times or delays corresponding to multiple transmission paths and targets, respectively. Prior works addressed recovery of unknown channels and signals in this ill-posed DBD problem through atomic norm minimization but contingent on *individual* minimum separation conditions for radar and communications channels. In this paper, we provide an optimal *joint* separation condition using extremal functions from the Beurling-Selberg interpolation theory. Thereafter, we formulate DBD as a low-rank modified Hankel matrix retrieval and solve it via nuclear norm minimization. We estimate the unknown target and communications parameters from the recovered low-rank matrix using *multiple signal classification* (MUSIC) method. We show that the joint separation condition also guarantees that the underlying Vandermonde matrix for MUSIC is well-conditioned. Numerical experiments validate our theoretical findings.

Index Terms—Beurling-Selberg majorant, condition number, dual-blind deconvolution, joint radar-communications, passive radar.

I. INTRODUCTION

The electromagnetic spectrum is a scarce natural resource. With the advent of cellular communications and novel radar applications, the spectrum has become increasingly contested. This has led to the development of joint radar-communications (JRC) systems, which facilitate spectrum-sharing while offering benefits of low cost, compact size, and less power consumption [1–4]. The JRC design topologies broadly fall into three categories: co-design [5], cooperation [6], and co-existence [7]. The spectral co-design employs a common transmit waveform and/or hardware while the cooperation technique relies on opportunistic processing of signals from one system to aid the other. The spectral co-existence is useful for legacy systems, wherein the radar and communications transmit and access the channel independently, receive overlaid signals at the receiver, and mitigate mutual interference. In this paper, we focus on the overlaid receiver for the spectral coexistence scenario.

This research was sponsored by the Army Research Office/Laboratory under Grant Number W911NF-21-1-0099, and the VIE project entitled “Dual blind deconvolution for joint radar-communications processing”. K. V. M. acknowledges support from the National Academies of Sciences, Engineering, and Medicine via the Army Research Laboratory Harry Diamond Distinguished Fellowship.

In conventional radar applications, the transmit waveform is known to the receiver and the goal of signal processing is to extract the unknown target parameters. In wireless communications, the roles are reversed with the channel estimated *a priori* and the receiver estimating the unknown transmit messages. In certain applications, both signals and channels may be unknown to the receiver. For instance, passive [8] and multistatic [9] radars employed for low-cost and efficient covert operations are generally not aware of the transmit waveform [10]. In mobile radio [11] and vehicular [12] communications, the channel is highly dynamic and any prior estimates may be inaccurate. A common receiver [13] in this general spectral coexistence scenario, therefore, deals with unknown radar and communications channels and their respective unknown transmit signals.

Prior works modeled the extraction of all four of these quantities, i.e. radar and communications channels and signals, as a *dual-blind deconvolution* (DBD) problem [14–17]. Herein, the observation is a sum of two convolutions and all four signals being convolved need to be estimated. This formulation is related to (single-)blind deconvolution (BD), a longstanding problem that occurs in a variety of engineering and scientific applications [18–20]. The DBD problem is highly ill-posed. In [15], authors leveraged upon the sparsity of radar and communications channels to recast DBD as the minimization of the sum of multivariate atomic norms (SoMAN). The ANM facilitates recovering continuous-valued parameters [21–23]. Using the theories of positive hyperoctant polynomials, they then devised a semidefinite program (SDP) for SoMAN and estimated the unknown target and communications parameters.

The SoMAN approach guarantees perfect DBD recovery assuming individual minimum separation conditions of the spikes (or targets) in the radar and communications channels [15]. In this paper, we provide an improved guarantee by suggesting a joint minimum separation. In particular, we focus on delay-only DBD and rely on relating the extremal functions in the Beurling-Selberg interpolation theory [24–27] to the spectral properties of an entry-wise weighted Vandermonde matrix that results from the decomposition of the vectorized Hankel matrix. We employ the Beurling-Selberg majorant and minorant functions of the interval function on the real line because they are compactly supported on the Fourier domain. The connection between extremal functions and the condition number of Vandermonde matrices was earlier studied by [28] in the context of (non-blind) super-resolution.

Contrary to the SoMAN formulation that exploits channel sparsity, our approach is based on nuclear norm minimization to recover a low-rank vectorized Hankel matrix, from which unknown target and communications parameters are estimated by the *multiple signal classification* (MUSIC) algorithm [29]. The low-rankness of radar/communications receive signals has been previously validated in related applications such as super-resolution of complex exponentials [30] and multipath channels in wireless communications [31, 32]. In this work, our joint separation condition guarantees a well-conditioned Vandermonde matrix – shown to be low-rank in

a sliding column form [33] – for MUSIC-based recovery.

This paper uses boldface lowercase and uppercase for vectors and matrices, respectively. The i -th entry of the vector \mathbf{x} is $[\mathbf{x}]_i$, $[\mathbf{X}]_{i,j}$ represents the i -th row and j -th column of \mathbf{X} . \mathbf{x}_r is the i -th column of \mathbf{X}_r . We denote the transpose, conjugate, and Hermitian by $(\cdot)^T$, $(\cdot)^*$, and $(\cdot)^H$, respectively. Unless otherwise specified, the integrals and summation limits are $-\infty$ and ∞ . The functions $\max(a,b)$ and $\min(a,b)$ return, respectively, maximum and minimum of the input arguments. The expression $\sum_{i,i'=1}^{K,Q} a_i b_{i'} = \sum_{i=1}^K \sum_{i'=1}^Q a_i b_{i'}$. \mathcal{F} represents the continuous-time Fourier transform (CTFT); $*$ denotes the convolution operation; $\langle \mathbf{A}, \mathbf{B} \rangle = \text{Tr}(\mathbf{A}^* \mathbf{B})$, and $\text{Tr}(\cdot)$ is the matrix trace; $\sigma_{\min}(\mathbf{A})$ is the minimum singular value of \mathbf{A} ; and $\text{rank}(\mathbf{A})$ is its matrix rank.

II. SIGNAL MODEL

Consider a radar that transmits a time-limited baseband pulse $g_r(t)$, whose CTFT is $\tilde{g}_r(f) = \int g_r(t) e^{-j2\pi f t} dt$, assuming that most of the radar signal's energy lies within the frequencies $\pm B/2$ yields to $g_r(f) \approx \int_{-B/2}^{B/2} g_r(t) e^{-j2\pi f t} dt$. The pulse $g_r(t)$ is reflected back to the receiver by K targets, where the i -th target is characterized by time delay $[\tau_r]_i$ and complex amplitude $[\beta]_i$. $[\tau_r]_i$ is linearly proportional to the target's range and $[\beta]_i$ models the path loss and reflectivity. The radar channel is

$$h_r(t) = \sum_{i=0}^{K-1} [\beta]_i \delta(t - [\tau_r]_i). \quad (1)$$

The communications transmitted signal $g_c(t)$ is a message modeled as an orthogonal frequency-division multiplexing (OFDM) signal with bandwidth B and M equi-bandwidth sub-carriers separated by Δf , i.e.,

$$g_c(t) = \sum_{l=1}^M [\tilde{\mathbf{g}}_c]_l e^{j2\pi l \Delta f t}, \quad (2)$$

where $[\tilde{\mathbf{g}}_c]_l$ is the modulated symbol onto the l -th subcarrier. The message propagates through a communications channel $h_c(t)$ that comprises Q paths characterized by their attenuation/channel coefficients $\boldsymbol{\omega} \in \mathbb{C}^Q$ and delays $\boldsymbol{\tau}_c \in \mathbb{C}^Q$:

$$h_c(t) = \sum_{q=1}^Q [\boldsymbol{\omega}]_q \delta(t - [\tau_c]_q). \quad (3)$$

The radar and communications systems share the spectrum in a spectral coexistence scenario. The common received signal is a superposition of radar and communications signals propagated through their respective channels as

$$\begin{aligned} y(t) &= g_r(t) * h_r(t) + g_c(t) * h_c(t), \\ &= \sum_{i=1}^K [\beta]_i g_r(t - [\tau_r]_i) + \sum_{q=1}^Q [\boldsymbol{\omega}]_q g_c(t - [\tau_c]_q). \end{aligned} \quad (4)$$

The CTFT of the overlaid signal is

$$Y(f) = \sum_{i=1}^K [\beta]_i e^{-j2\pi[\tau_r]_i f} \tilde{g}_r(f) + \sum_{q=1}^Q [\boldsymbol{\omega}]_q e^{-j2\pi[\tau_c]_q f} \tilde{g}_c(f), \quad (5)$$

where $\tilde{g}_c(f) = \mathcal{F}\{g_c(t)\}$. Sampling (5) at the Nyquist rate of $\Delta_f = \frac{B}{N}$, where $n = 0, \dots, N-1$, yields

$$\begin{aligned} Y(n) &= \sum_{i=1}^K [\beta]_i e^{-j2\pi[\tau_r]_i n \Delta_f} \tilde{g}_r(n \Delta_f) \\ &\quad + \sum_{q=1}^Q [\boldsymbol{\omega}]_q e^{-j2\pi[\tau_c]_q n \Delta_f} \tilde{g}_c(n \Delta_f). \end{aligned} \quad (6)$$

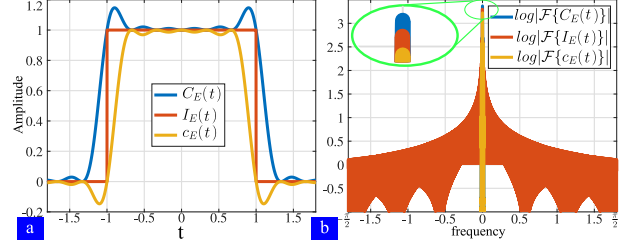


Fig. 1. (a) Beurling-Selberg majorant (blue) and minorant (orange) functions and the indicator function $I_E(t)$ (red) for the interval $E = [-1, 1]$. (b) Fourier transform of $C_E(t)$ (blue), $I_E(t)$ (red), and $c_E(t)$ (orange) on log-absolute-value scale.

Collect the samples of $\tilde{g}_r(n\Delta_f)$ in the vector $\tilde{\mathbf{g}}_r$, i.e., $[\tilde{\mathbf{g}}_r]_n = \tilde{g}_r(n\Delta_f)$. Similarly, $\tilde{g}_c(n\Delta_f) = [\tilde{\mathbf{g}}_c]_n$. The samples $[\mathbf{y}]_n = Y(n)$ of the observation vector \mathbf{y} are

$$[\mathbf{y}]_n = \sum_{i=1}^K [\beta]_i e^{-j2\pi[\tau_r]_i n} [\tilde{\mathbf{g}}_r]_n + \sum_{q=1}^Q [\boldsymbol{\omega}]_q e^{-j2\pi[\tau_c]_i n} [\tilde{\mathbf{g}}_c]_n. \quad (7)$$

Our goal in the DBD problem is to estimate the parameters $\boldsymbol{\tau}_r$, $\boldsymbol{\tau}_c$, $\boldsymbol{\beta}$, and $\boldsymbol{\omega}$ from \mathbf{y} , without knowledge of the radar pulse $\tilde{\mathbf{g}}_r$ or communications symbols $\tilde{\mathbf{g}}_c$. This is an ill-posed problem because of many unknown variables and fewer measurements. Finally, the problem can be expressed in matrix form by denoting $\alpha_{[\tau_r]_i}^n = e^{-j2\pi n [\tau_r]_i}$, $\alpha_{[\tau_c]_l}^n = e^{-j2\pi n [\tau_c]_l}$, and $\boldsymbol{\psi} = [\boldsymbol{\beta}^T, \boldsymbol{\omega}^T]^T$. Rewrite the overlaid receiver signal in (7) as a linear system:

$$\begin{aligned} \mathbf{y} &= \begin{bmatrix} [\tilde{\mathbf{g}}_r]_0 & \dots & [\tilde{\mathbf{g}}_r]_1 & \dots & [\tilde{\mathbf{g}}_c]_1 & \dots & [\tilde{\mathbf{g}}_c]_1 \\ [\tilde{\mathbf{g}}_r]_2 \alpha_{[\tau_r]_1}^1 & \dots & [\tilde{\mathbf{g}}_r]_2 \alpha_{[\tau_r]_K}^1 & \dots & [\tilde{\mathbf{g}}_c]_2 \alpha_{[\tau_c]_1}^1 & \dots & [\tilde{\mathbf{g}}_c]_2 \alpha_{[\tau_c]_Q}^1 \\ \vdots & \vdots & \vdots & \vdots & \vdots & \vdots & \vdots \\ [\tilde{\mathbf{g}}_r]_N \alpha_{[\tau_r]_1}^N & \dots & [\tilde{\mathbf{g}}_r]_N \alpha_{[\tau_r]_K}^N & \dots & [\tilde{\mathbf{g}}_c]_N \alpha_{[\tau_c]_1}^N & \dots & [\tilde{\mathbf{g}}_c]_N \alpha_{[\tau_c]_Q}^N \end{bmatrix} \boldsymbol{\psi} \\ &= \text{diag}(\mathbf{g}_r) \mathbf{V}_r \boldsymbol{\beta} + \text{diag}(\mathbf{g}_c) \mathbf{V}_c \boldsymbol{\omega} = \mathbf{V}_g \boldsymbol{\psi}, \end{aligned} \quad (8)$$

where \mathbf{V}_r and \mathbf{V}_c are Vandermonde matrices such that $[\mathbf{V}_r]_{l,i} = \alpha_{[\tau_r]_i}^l$ and $[\mathbf{V}_c]_{l,l} = \alpha_{[\tau_c]_l}^l$.

III. BEURLING-SELBERG EXTREMAL FUNCTIONS

The guarantees to DBD recovery in previous studies [14] are based on the minimum separation of spikes in each channel assuming a noiseless scenario. Here, we resort to the Beurling-Selberg extremal functions to derive an optimal separation condition that imposes a joint structure on the two channels. This result follows analyzing the condition number of \mathbf{V}_g that controls the stability of the solution of (8) in the presence of additive noise.

Consider the indicator function $I_E(t)$ defined on the interval $[0, N-1]$, where $I_E(t)$ equals 1 if $0 < t < N-1$, and 0 otherwise. We can find approximations for $I_E(t)$ using functions $b(t)$ and $B(t)$ such that $b(t) \leq I_E(t) \leq B(t)$. Moreover, we seek to minimize the integrals $\int (B(t) - I_E(t)) dt$ and $\int (I_E(t) - b(t)) dt$. These optimization problems are known as extremal problems, and the resulting functions $C_E(t)$ (majorant) and $c_E(t)$ (minorant) are considered extremal functions.

Beurling [26, 34] found a solution to this extremal problem for the sign function by restricting $C_E(t)$ and $c_E(t)$ to be real entire functions of exponential type 2π . Recall that if an entire function $F: \mathbb{C}^N \rightarrow \mathbb{C}$ is real-valued when it is restricted to \mathbb{R}^N , it is called a real entire function. Additionally, if this statement holds and the growth of F is bounded by a constant C and $Ce^{(2\pi+\epsilon)|z|}$ for every $\epsilon > 0$, $z \in \mathbb{C}$, it is called a real entire function of exponential type 2π . Selberg observed that Beurling functions can majorize and minorize the characteristic function $I_E(t)$. The resultant majorant and minorant functions have the useful property that their Fourier transforms are continuous functions supported on

the interval $[-\Delta, \Delta]$ [24–27]. We intend to employ these functions to provide a bound on the \mathbf{V}_g condition number. Fig. 1a shows that these functions approximate and bound the indicator function as $C_E(t) \leq I_E(t) \leq c_E(t)$. Fig. 1b depicts these functions in the Fourier domain. To this end, define the separation between the delay parameters corresponding to radar-only, communications-only and radar-communications measurements as, respectively, $\gamma_{i,i'} = |[\boldsymbol{\tau}_r]_i - [\boldsymbol{\tau}_r]_{i'}|$, $\zeta_{i,i'} = |[\boldsymbol{\tau}_c]_i - [\boldsymbol{\tau}_c]_{i'}|$, and $\xi_{i,i'} = |[\boldsymbol{\tau}_r]_i - [\boldsymbol{\tau}_c]_{i'}|$. Denote $\Delta_r = \min_{i \neq i'} \gamma_{i,i'}$, $\Delta_c = \min_{i \neq i'} \zeta_{i,i'}$, $\Delta_{rc} = \min_{i, i'} \xi_{i,i'}$, and $\Delta = \min(\Delta_r, \Delta_c, \Delta_{rc})$. The following Proposition 1 states that the condition number is governed by the number of samples and the joint minimum separation.

Proposition 1. *The condition number κ_g of matrix \mathbf{V}_g in (8) satisfies $\kappa_g^2 \leq (N - 1/\Delta + 1)/(N - 1/\Delta - 1)$.*

Proof: Recall the received signal in (8). Consider the Dirac comb $h(n) = \sum_t \delta(n - t) = \sum_{t'} e^{j2\pi t' n}$. The norm of the measurements is

$$\begin{aligned} \sum_{n=0}^{N-1} \|\mathbf{y}_n\|^2 &= \int h(n) I_E(n) \|Y(n)\|^2 \partial n \\ &\leq \int h(n) C_E(n) \|Y(n)\|^2 \partial n = \int h(n) C_E(n) Y(n) Y^*(n) \partial n \\ &= \left(\sum_{i,i'=1}^K [\boldsymbol{\beta}]_i [\boldsymbol{\beta}]_{i'}^* \int h(n) C_E(n) |\tilde{g}_r(n)|^2 \alpha_{\gamma_{i,i'}}^n \partial n \right. \\ &+ \sum_{i,i'=1}^{K,Q} [\boldsymbol{\beta}]_i [\boldsymbol{\omega}]_{i'}^* \int h(n) C_E(n) \tilde{g}_r(n) \tilde{g}_c^*(n) \alpha_{\gamma_{i,i'}}^n \partial n \\ &+ \sum_{i,i'=1}^{Q,K} [\boldsymbol{\omega}]_i [\boldsymbol{\beta}]_{i'}^* \int h(n) C_E(n) \tilde{g}_r^*(n) \tilde{g}_c(n) \alpha_{\xi_{i,i'}}^n \partial n \\ &\left. + \sum_{i,i'=1}^Q [\boldsymbol{\omega}]_i [\boldsymbol{\omega}]_{i'}^* \int h(n) C_E(n) |\tilde{g}_c(n)|^2 \alpha_{\zeta_{i,i'}}^n \partial n \right), \end{aligned} \quad (9)$$

where the inequality follows from replacing $I_E(n)$ by $C_E(n)$. Substituting the expression of the Dirac comb $h(n)$, $g_{r,c}(n) = \tilde{g}_r(n) \tilde{g}_c^*(n)$, and $g_{c,r}(n) = \tilde{g}_c(n) \tilde{g}_r^*(n)$ produces

$$\begin{aligned} \sum_{n=0}^{N-1} \|\mathbf{y}_n\|^2 &\leq \left(\sum_{i'} \sum_{i,i'=1}^K [\boldsymbol{\beta}]_i [\boldsymbol{\beta}]_{i'}^* \mathcal{F} \left\{ C_E(n) |\tilde{g}_r(n)|^2 \alpha_{\gamma_{i,i'}}^n \right\} \right. \\ &+ \sum_{t'} \sum_{i,i'=1}^{K,Q} [\boldsymbol{\beta}]_i [\boldsymbol{\omega}]_{i'}^* \mathcal{F} \left\{ C_E(n) g_{r,c}(n) \alpha_{\xi_{i,i'}}^n \right\} \\ &+ \sum_{t'} \sum_{i,i'=1}^{Q,K} [\boldsymbol{\omega}]_i [\boldsymbol{\beta}]_{i'}^* \mathcal{F} \left\{ C_E(n) g_{c,r}(n) \alpha_{\xi_{i,i'}}^n \right\} \\ &\left. + \sum_{t'} \sum_{i,i'=1}^Q [\boldsymbol{\omega}]_i [\boldsymbol{\omega}]_{i'}^* \mathcal{F} \left\{ C_E(n) |\tilde{g}_c(n)|^2 \alpha_{\zeta_{i,i'}}^n \right\} \right). \end{aligned} \quad (10)$$

Using the convolution theorem and $\tilde{C}_E = \mathcal{F}\{C_E\}$ yields

$$\begin{aligned} \|\mathbf{y}_n\|^2 &\leq \left(\sum_{t'} \sum_{i,i'=1}^K [\boldsymbol{\beta}]_i [\boldsymbol{\beta}]_{i'}^* \tilde{C}_E(t' + \gamma_{i,i'}) * \mathcal{F} \left\{ \tilde{g}_r(n)^2 \alpha_{\gamma_{i,i'}}^n \right\} \right. \\ &+ \sum_{t'} \sum_{i,i'=1}^{K,Q} [\boldsymbol{\beta}]_i [\boldsymbol{\omega}]_{i'}^* \tilde{C}_E(t' + \xi_{i,i'}) * \mathcal{F} \left\{ g_{r,c}(n) \alpha_{\xi_{i,i'}}^n \right\} \\ &\left. + \sum_{t'} \sum_{i,i'=1}^{Q,K} [\boldsymbol{\omega}]_i [\boldsymbol{\beta}]_{i'}^* \tilde{C}_E(t' + \xi_{i,i'}) * \mathcal{F} \left\{ g_{c,r}(n) \alpha_{\xi_{i,i'}}^n \right\} \right. \\ &\left. + \sum_{t'} \sum_{i,i'=1}^Q [\boldsymbol{\omega}]_i [\boldsymbol{\omega}]_{i'}^* \tilde{C}_E(t' + \zeta_{i,i'}) * \mathcal{F} \left\{ |\tilde{g}_c(n)|^2 \alpha_{\zeta_{i,i'}}^n \right\} \right). \end{aligned} \quad (11)$$

$$\begin{aligned} &+ \sum_{t'} \sum_{i,i'=1}^{Q,K} [\boldsymbol{\omega}]_i [\boldsymbol{\beta}]_{i'}^* \tilde{C}_E(t' + \xi_{i,i'}) * \mathcal{F} \left\{ g_{c,r}(n) \alpha_{\xi_{i,i'}}^n \right\} \\ &+ \sum_{t'} \sum_{i,i'=1}^Q [\boldsymbol{\omega}]_i [\boldsymbol{\omega}]_{i'}^* \tilde{C}_E(t' + \zeta_{i,i'}) * \mathcal{F} \left\{ |\tilde{g}_c(n)|^2 \alpha_{\zeta_{i,i'}}^n \right\}. \end{aligned}$$

Note that \tilde{C}_E is supported on $[-\Delta, \Delta]$. Hence, the first and fourth terms are non-zero only when $t' = 0$ and $i = i'$. The second and third terms are zero for all t', i, i' because $|t' + \xi_{i,i'}| > \Delta$, for all t', i, i' . Substituting $G_{ri}(n) = |\beta_i|^2 \mathcal{F}\{|\tilde{g}_r(n)|^2 \alpha_{\gamma_{i,i}}^n\}$, $G_{ci}(n) = |\omega_i|^2 \mathcal{F}\{|\tilde{g}_c(n)|^2 \alpha_{\zeta_{i,i}}^n\}$ in (12) yields

$$\|\mathbf{y}_n\|^2 \leq \sum_i^K \tilde{C}_E(0) * G_{ri}(n) + \sum_i^Q \tilde{C}_E(0) * G_{ci}(n). \quad (12)$$

From [28, Theorem 2.2], the integral of the majorant function, i.e., $\int C_E(t) = 2n + 1/\Delta$. Hence, we obtain

$$\|\mathbf{V}_g \boldsymbol{\psi}\|^2 = \sum_{n=0}^{N-1} \|\mathbf{y}_n\|^2 \leq (2n + \frac{1}{\Delta}) \times G(n), \quad (13)$$

where $G(n) = \sum_i^K G_{ri}(n) + \sum_i^Q G_{ci}(n)$. The lower bound is similarly obtained from the minorant $c_E(n)$, whose Fourier transform is supported on $[-\Delta, \Delta]$, as

$$\|\mathbf{V}_g \boldsymbol{\psi}\|^2 = \sum_{n=0}^{N-1} \|\mathbf{y}_n\|^2 \geq (2n - \frac{1}{\Delta}) \times G(n), \quad (14)$$

Defining $\kappa_g^2 = (\max_{\nu} \|\mathbf{V}_g \boldsymbol{\nu}\|^2 / \min_{\nu} \|\mathbf{V}_g \boldsymbol{\nu}\|^2)$ and $N = 2n + 1$ results in $\kappa_g^2 \leq (N + \frac{1}{\Delta} - 1) / (N - \frac{1}{\Delta} - 1)$. ■

From Proposition 1, the condition number depends on the minimum joint separation. This gives $N > (1/\Delta + 1)$, this shows the coupled nature of radar and communications in the DBD problem.

IV. LOW-RANK HANKEL MATRIX RECOVERY

The recovery of $\boldsymbol{\tau}_r$, $\boldsymbol{\tau}_c$, $\boldsymbol{\beta}$, and $\boldsymbol{\omega}$ poses challenges due to the ill-posed nature of the problem. To address this, we reasonably assume that the unknown point spread functions (PSF), \mathbf{g}_r and \mathbf{g}_c , can be accurately represented within a known low-dimensional subspace. This assumption is justified by considering the rank of the Vandermonde matrices, which is influenced by the number of radar and communications delays which is usually smaller than the number of measurements [13–15, 29]. Following this, we denote $\tilde{\mathbf{g}}_r = \mathbf{B} \mathbf{h}_r$ and $\tilde{\mathbf{g}}_c = \mathbf{D} \mathbf{h}_c$, where $\mathbf{B} \in \mathbb{C}^{N_r \times N_r}$, $\mathbf{h}_r \in \mathbb{C}^{N_r}$, $\mathbf{D} \in \mathbb{C}^{N_c \times N_c}$, and $\mathbf{h}_c \in \mathbb{C}^{N_c}$. Collect the unknown radar and communications variables, respectively, in the matrices $\mathbf{X}_r = \sum_{i=1}^K [\boldsymbol{\beta}]_i \mathbf{h}_r \mathbf{a}_{[\boldsymbol{\tau}_r]_i}^T \in \mathbb{C}^{N_r \times N}$ and $\mathbf{X}_c = \sum_{i=1}^Q [\boldsymbol{\omega}]_i \mathbf{h}_c \mathbf{a}_{[\boldsymbol{\tau}_c]_i}^T \in \mathbb{C}^{N_c \times N}$, with $\mathbf{a}_{[\boldsymbol{\tau}_r]_i}^T = [1, e^{-j2\pi[\boldsymbol{\tau}_r]_i}, e^{-j2\pi[\boldsymbol{\tau}_r]_i(2)}, \dots, e^{-j2\pi[\boldsymbol{\tau}_r]_i(N-1)}]$ is the vector containing all the atoms $\alpha_{[\boldsymbol{\tau}_r]_i}^n$; $\mathbf{a}_{[\boldsymbol{\tau}_c]_i}^T$ is defined similarly using atoms $\alpha_{[\boldsymbol{\tau}_c]_i}^n$. Denote $\mathbf{s}_j = [\mathbf{b}_j, \mathbf{d}_j^T]^T$, where \mathbf{b}_j and \mathbf{d}_j are the j -th columns of \mathbf{B}^* and \mathbf{D}^* , respectively. Rewrite (7) as

$$\mathbf{y}_j = \langle \mathbf{s}_j \mathbf{e}_j^T, \mathbf{X} \rangle, \quad (15)$$

with $\mathbf{X} = [\mathbf{X}_r^T, \mathbf{X}_c^T]^T \in \mathbb{C}^{(N_r+N_c) \times N}$, and $\mathbf{e}_j \in \mathbb{R}^N$ is the j -th canonical vector. For the sake of simplicity, consider $N_c = N_r = N_{rc}$. Define a linear operator $\mathcal{A} : \mathbb{C}^{2N_{rc} \times N} \rightarrow \mathbb{C}^N$ such that $[\mathcal{A}(\mathbf{X})]_j = \langle \mathbf{s}_j \mathbf{e}_j^T, \mathbf{X} \rangle$. Then, (15) becomes

$$\mathbf{y} = \mathcal{A}(\mathbf{X}). \quad (16)$$

Select $N_1, N_2 \in \mathbb{N}$ such that $N_1 + N_2 = N + 1$. The low-dimensional subspace assumption allows us to represent the unknown variables in a low-rank matrix. To construct such a matrix, apply a linear operator $\mathcal{H}(\cdot)$ to both \mathbf{X}_r and \mathbf{X}_c such that it

produces a Hankel matrix of higher dimensions using the columns of the input matrix. Then, concatenating both Hankel matrices using the operator $\mathcal{C}(\mathbf{X}) = \mathcal{C}([\mathbf{X}_r^T, \mathbf{X}_c^T]^T) = [\mathcal{H}(\mathbf{X}_r), \mathcal{H}(\mathbf{X}_c)]$ yields

$$\mathcal{C}(\mathbf{X}) = \begin{bmatrix} \mathbf{x}_{r0} & \dots & \mathbf{x}_{rN_2-1} & \mathbf{x}_{c0} & \dots & \mathbf{x}_{cN_2-1} \\ \mathbf{x}_{r1} & \dots & \mathbf{x}_{rN_2} & \mathbf{x}_{c1} & \dots & \mathbf{x}_{cN_2} \\ \vdots & & \vdots & \vdots & & \vdots \\ \mathbf{x}_{rN_1-1} & \dots & \mathbf{x}_{rN_1} & \mathbf{x}_{cN_1-1} & \dots & \mathbf{x}_{cN_1} \end{bmatrix}. \quad (17)$$

The concatenated matrix is decomposed as

$$\mathcal{C}(\mathbf{X}) = \mathbf{V}_{h,\alpha} \text{diag}(\boldsymbol{\psi}) \mathbf{V}_\alpha^T, \quad (18)$$

where the $(N_1 N_{rc}) \times (K + Q)$ complex matrix $\mathbf{V}_{h,\alpha}$ is

$$\mathbf{V}_{h,\alpha} = \begin{bmatrix} \mathbf{h}_r & \dots & \mathbf{h}_r & \mathbf{h}_c & \dots & \mathbf{h}_c \\ \mathbf{h}_r \alpha_{[\tau_r]_1}^1 & \dots & \mathbf{h}_r \alpha_{[\tau_r]_K}^1 & \mathbf{h}_c \alpha_{[\tau_c]_1}^1 & \dots & \mathbf{h}_c \alpha_{[\tau_c]_Q}^1 \\ \vdots & & \vdots & \vdots & & \vdots \\ \mathbf{h}_r \alpha_{[\tau_r]_1}^{N_1-1} & \dots & \mathbf{h}_r \alpha_{[\tau_r]_K}^{N_1-1} & \mathbf{h}_c \alpha_{[\tau_c]_1}^{N_1-1} & \dots & \mathbf{h}_c \alpha_{[\tau_c]_Q}^{N_1-1} \end{bmatrix}, \quad (19)$$

with $\alpha_{[\tau_r]_i}^{n_1}$ and $\alpha_{[\tau_c]_l}^{n_1}$ are as defined in (8) except that $n_1 = 0, \dots, N_1 - 1$ and $n_2 = 0, \dots, N_2 - 1$, and

$$\mathbf{V}_\alpha^T = \begin{bmatrix} \alpha_r^0 & \dots & \alpha_r^{N_2-1} & 0 & \dots & 0 \\ 0 & \dots & 0 & \alpha_c^0 & \dots & \alpha_c^{N_2-1} \end{bmatrix}, \in \mathbb{R}^{(K+Q) \times 2N_2}, \quad (20)$$

with $\boldsymbol{\alpha}_r^{n_2} = [e^{-j2\pi n_2[\tau_r]_1}, e^{-j2\pi n_2[\tau_r]_2}, \dots, e^{-j2\pi n_2[\tau_r]_K}]^T \in \mathbb{R}^K$ and $\boldsymbol{\alpha}_c^{n_2} = [e^{-j2\pi n_2[\tau_c]_1}, e^{-j2\pi n_2[\tau_c]_2}, \dots, e^{-j2\pi n_2[\tau_c]_Q}]^T \in \mathbb{R}^Q$.

From (18), $\text{rank}(\mathcal{C}(\mathbf{X})) \leq (K + Q)$. Hence, $\mathcal{C}(\mathbf{X})$ is a low-rank structure. Then, the problem of recovering \mathbf{X} becomes

$$\underset{\mathbf{X} \in \mathbb{R}^{2 \times N_{rc} \times N}}{\text{argmin}} \|\mathcal{C}(\mathbf{X})\|_* \text{ subject to } \mathbf{y} = \mathcal{A}(\mathbf{X}). \quad (21)$$

An optimal solution to (21) is guaranteed [29] if $\sigma_{\min}(\mathbf{V}_{h,\alpha} \mathbf{V}_{h,\alpha}^T) \geq N_1/\mu$ and $\sigma_{\min}(\mathbf{V}_\alpha \mathbf{V}_\alpha^T) \geq N_2/\mu$ for $\mu > 1$. From Proposition 1 and [29], these conditions imply $\Delta > 2\mu/N(\mu - 1)$. Once the matrix \mathbf{X} is obtained, the delays $\boldsymbol{\tau}_r, \boldsymbol{\tau}_c$ are recovered via MUSIC. Finally, the waveforms $\mathbf{g}_r, \mathbf{g}_c$ are retrieved using the least-squares method [14].

V. NUMERICAL EXPERIMENTS

We compared our approach to DBD against SoMAN SDP in [14], which assumes a low-dimensional subspace structure of the waveform \mathbf{g}_r and message \mathbf{g}_c and additionally exploits the sparsity of the channels. The SoMAN method represents the matrices \mathbf{X}_r and \mathbf{X}_c as a linear combination of atoms given by the sets $\mathcal{A}_r = \{\mathbf{h}_r \mathbf{a}_{\tau_r}^H : \tau_r \in [0, 1)\}$ and $\mathcal{A}_c = \{\mathbf{h}_c \mathbf{a}_{\tau_c}^H, \tau_c \in [0, 1)\} \subset \mathbb{C}^{N_{rc} \times N}$. This leads to the following formulation of *atomic norms*

$$\|\mathbf{X}_r\|_{\mathcal{A}_r} = \inf \left\{ \sum_{\ell} |\beta|_{\ell} \left| \mathbf{X}_r = \sum_{\ell} [\beta]_{\ell} \mathbf{h}_r \mathbf{a}_{\tau_r}^H \right| \right\}, \quad (22)$$

$$\|\mathbf{X}_c\|_{\mathcal{A}_c} = \inf \left\{ \sum_q |\omega|_q \left| \mathbf{X}_c = \sum_q [\omega]_q \mathbf{h}_c \mathbf{a}_{\tau_c}^H \right| \right\}. \quad (23)$$

The SoMAN minimization estimates \mathbf{X}_r and \mathbf{X}_c as

$$\min_{\mathbf{X}_r, \mathbf{X}_c} \|\mathbf{X}_r\|_{\mathcal{A}_r} + \|\mathbf{X}_c\|_{\mathcal{A}_c} \text{ s. t. } \mathbf{y} = \mathfrak{N}_r(\mathbf{X}_r) + \mathfrak{N}_c(\mathbf{X}_c). \quad (24)$$

where $[\mathfrak{N}_r(\mathbf{X}_r)]_i = \text{Tr}(\mathbf{e}_i \mathbf{h}_r^H \mathbf{X}_r)$ and $[\mathfrak{N}_c(\mathbf{X}_c)]_j = \text{Tr}(\mathbf{e}_j \mathbf{h}_c^H \mathbf{X}_c)$.

To evaluate the performance of the proposed vectorized Hankel method, we performed several computational simulations using CVX [35, 36] library in MATLAB with SDPT3 [37] solver. The delays $\boldsymbol{\tau}_r$ and $\boldsymbol{\tau}_c$ were drawn uniformly at random from the interval $[0, 1)$; the amplitudes $\boldsymbol{\beta}, \boldsymbol{\omega}$ were generated following $(1+10^\gamma)e^{-j\phi}$ with γ sampled from a uniform distribution $[0, 1)$ and ϕ from

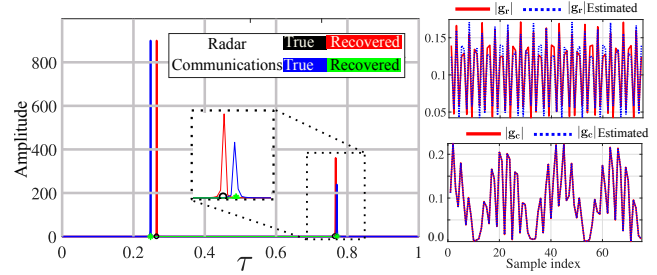


Fig. 2. The pseudo-spectrum computed using the MUSIC algorithm and the true radar $\boldsymbol{\tau}_r$ and communications $\boldsymbol{\tau}_c$ delays (left), recovered radar waveform (right top), and communications message (right bottom) with $N = 75$ samples, $K = 2$ targets and $Q = 2$ paths and subspace dimensions $N_r = N_c = 2$. The NMSE obtained is 0.09987 and $2.3144e-5$ for the radar waveform \mathbf{g}_r (top-right) and communications message \mathbf{g}_c (bottom-right), respectively.

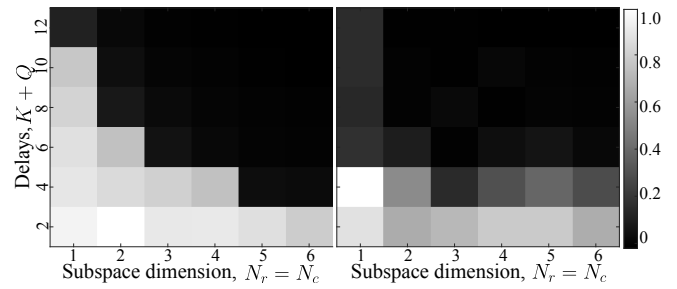


Fig. 3. The probability of reconstruction, averaged over 20 realizations with $N = 75$, for the proposed modified Hankel matrix recovery (left) and SoMAN SDP (right).

$[0, 2\pi)$. The columns of the matrices \mathbf{B} and \mathbf{D} are random columns of the DFT matrix of the corresponding size.

Figure 2 shows a specific delay recovery with two radar targets, two communication paths, and two unknown PSFs with $N_r = N_c = 2$, $K = Q = 2$, and 75 samples. The pseudospectrum is computed using MUSIC [29]. The proposed method is able to recover the exact position of the delays. Additionally, the recovered radar waveform and communications message are accurately estimated with the normalized mean-squared error (NMSE) $= \|\mathbf{g} - \mathbf{g}^*\| / \|\mathbf{g}\|$ of 0.0998 and 2.31×10^{-5} respectively. Figure 3 shows the reconstruction probability of the matrices \mathbf{X}_r and \mathbf{X}_c over 20 experiments, where success is declared if the NMSE between the truth and recovered \mathbf{X} is lower than 10^{-3} . We observe that the phase transition curve of the proposed method is higher than the SoMAN approach.

VI. SUMMARY

We provided an optimal separation condition for the DBD problem using extremization functions. This condition depends on the separation of the radar and communications delays and, contrary to prior guarantees, is jointly imposed. Our recovery algorithm based on a modified vectorized Hankel matrix recovery outperforms SoMAN SDP. Future investigations require generalizing the proposed approach to other coexistence models considered in [14].

VII. REFERENCES

- [1] K. V. Mishra, M. R. Bhavani Shankar, V. Koivunen, B. Ottersten, and S. A. Vorobyov, "Toward millimeter wave joint radar-communications: A signal processing perspective," *IEEE Signal Processing Magazine*, vol. 36, no. 5, pp. 100–114, 2019.
- [2] G. Duggal, S. Vishwakarma, K. V. Mishra, and S. S. Ram, "Doppler-resilient 802.11ad-based ultrashort range automotive joint radar-communications system," *IEEE Transactions*

- on *Aerospace and Electronic Systems*, vol. 56, no. 5, pp. 4035–4048, 2020.
- [3] A. M. Elbir, K. V. Mishra, and S. Chatzinotas, “Terahertz-band joint ultra-massive MIMO radar-communications: Model-based and model-free hybrid beamforming,” *IEEE Journal of Special Topics in Signal Processing*, vol. 15, no. 6, pp. 1468–1483, 2021.
 - [4] A. M. Elbir, K. V. Mishra, M. R. B. Shankar, and S. Chatzinotas, “The rise of intelligent reflecting surfaces in integrated sensing and communications paradigms,” *arXiv preprint arXiv:2204.07265*, 2022.
 - [5] J. Liu, K. V. Mishra, and M. Saquib, “Co-designing statistical MIMO radar and in-band full-duplex multi-user MIMO communications,” *arXiv preprint arXiv:2006.14774*, 2020.
 - [6] M. Bicã and V. Koivunen, “Radar waveform optimization for target parameter estimation in cooperative radar-communications systems,” *IEEE Transactions on Aerospace and Electronic Systems*, vol. 55, no. 5, pp. 2314–2326, 2018.
 - [7] L. Wu, K. V. Mishra, M. R. Bhavani Shankar, and B. Ottersten, “Resource allocation in heterogeneously-distributed joint radar-communications under asynchronous Bayesian tracking framework,” *IEEE Journal on Selected Areas in Communications*, vol. 40, no. 7, pp. 2026–2042, 2022.
 - [8] S. Sedighi, K. V. Mishra, M. B. Shankar, and B. Ottersten, “Localization with one-bit passive radars in narrow-band internet-of-things using multivariate polynomial optimization,” *IEEE Transactions on Signal Processing*, vol. 69, pp. 2525–2540, 2021.
 - [9] S. H. Dokhanchi, B. S. Mysore, K. V. Mishra, and B. Ottersten, “A mmWave automotive joint radar-communications system,” *IEEE Transactions on Aerospace and Electronic Systems*, vol. 55, no. 3, pp. 1241–1260, 2019.
 - [10] H. Kuschel, D. Cristallini, and K. E. Olsen, “Passive radar tutorial,” *IEEE Aerospace and Electronic Systems Magazine*, vol. 34, no. 2, pp. 2–19, 2019.
 - [11] A. Neskovic, N. Neskovic, and G. Paunovic, “Modern approaches in modeling of mobile radio systems propagation environment,” *IEEE Communications Surveys & Tutorials*, vol. 3, no. 3, pp. 2–12, 2000.
 - [12] S. Olariu and M. C. Weigle, *Vehicular networks: From theory to practice*. Chapman and Hall/CRC, 2009.
 - [13] P. Vouras, K. V. Mishra, A. Artusio-Glimpse, S. Pinilla, A. Xenaki, D. W. Griffith, and K. Egiazarian, “An overview of advances in signal processing techniques for classical and quantum wideband synthetic apertures,” *arXiv preprint arXiv:2205.05602*, 2022.
 - [14] E. Vargas, K. V. Mishra, R. Jacome, B. M. Sadler, and H. Arguello, “Dual-blind deconvolution for overlaid radar-communications systems,” *IEEE Journal on Selected Areas in Information Theory*, 2023.
 - [15] —, “Joint radar-communications processing from a dual-blind deconvolution perspective,” in *IEEE International Conference on Acoustics, Speech and Signal Processing*, 2022, pp. 5622–5626.
 - [16] R. Jacome, K. V. Mishra, E. Vargas, B. M. Sadler, and H. Arguello, “Multi-dimensional dual-blind deconvolution approach toward joint radar-communications,” in *IEEE International Workshop on Signal Processing Advances in Wireless Communication*, 2022, pp. 1–5.
 - [17] R. Jacome, E. Vargas, K. V. Mishra, B. M. Sadler, and H. Arguello, “Factor graph processing for dual-blind deconvolution at ISAC receiver,” in *IEEE International Workshop on Computational Advances in Multi-Sensor Adaptive Processing*, 2023, in press.
 - [18] S. M. Jefferies and J. C. Christou, “Restoration of astronomical images by iterative blind deconvolution,” *The Astrophysical Journal*, vol. 415, p. 862, 1993.
 - [19] G. Ayers and J. C. Dainty, “Iterative blind deconvolution method and its applications,” *Optics Letters*, vol. 13, no. 7, pp. 547–549, 1988.
 - [20] K. Abed-Meraim, W. Qiu, and Y. Hua, “Blind system identification,” *Proceedings of the IEEE*, vol. 85, no. 8, pp. 1310–1322, 1997.
 - [21] B. N. Bhaskar, G. Tang, and B. Recht, “Atomic norm denoising with applications to line spectral estimation,” *IEEE Transactions on Signal Processing*, vol. 61, no. 23, pp. 5987–5999, 2013.
 - [22] K. V. Mishra, M. Cho, A. Kruger, and W. Xu, “Spectral super-resolution with prior knowledge,” *IEEE Transactions on Signal Processing*, vol. 63, no. 20, pp. 5342–5357, 2015.
 - [23] W. Xu, J.-F. Cai, K. V. Mishra, M. Cho, and A. Kruger, “Precise semidefinite programming formulation of atomic norm minimization for recovering d -dimensional ($d \geq 2$) off-the-grid frequencies,” in *IEEE Information Theory and Applications Workshop*, 2014, pp. 1–4.
 - [24] S. W. Graham and J. D. Vaaler, “A class of extremal functions for the fourier transform,” *Transactions of the American Mathematical Society*, vol. 265, no. 1, pp. 283–302, 1981.
 - [25] E. Carneiro, F. Littmann, and J. D. Vaaler, “Gaussian subordination for the beurling-selberg extremal problem,” *Transactions of the American Mathematical Society*, vol. 365, no. 7, pp. 3493–3534, 2013.
 - [26] E. Carneiro and J. D. Vaaler, “Some extremal functions in fourier analysis. ii,” *Transactions of the American Mathematical Society*, vol. 362, no. 11, pp. 5803–5843, 2010.
 - [27] E. Carneiro, “A survey on beurling-selberg majorants and some consequences of the riemann hypothesis,” *Matemática Contemporânea*, vol. 40, 2011.
 - [28] A. Moitra, “Super-resolution, extremal functions and the condition number of Vandermonde matrices,” in *Annual ACM symposium on Theory of computing*, 2015, pp. 821–830.
 - [29] J. Chen, W. Gao, S. Mao, and K. Wei, “Vectorized hankel lift: A convex approach for blind super-resolution of point sources,” *IEEE Transactions on Information Theory*, 2022.
 - [30] D. Yang, G. Tang, and M. B. Wakin, “Super-resolution of complex exponentials from modulations with unknown waveforms,” *IEEE Transactions on Information Theory*, vol. 62, no. 10, pp. 5809–5830, 2016.
 - [31] A. Ahmed, B. Recht, and J. Romberg, “Blind deconvolution using convex programming,” *IEEE Transactions on Information Theory*, vol. 60, no. 3, pp. 1711–1732, 2013.
 - [32] X. Luo and G. B. Giannakis, “Low-complexity blind synchronization and demodulation for (ultra-) wideband multi-user ad hoc access,” *IEEE Transactions on Wireless Communications*, vol. 5, no. 7, pp. 1930–1941, 2006.
 - [33] R. Heckel, V. I. Morgenshtern, and M. Soltanolkotabi, “Super-resolution radar,” *Information and Inference: A Journal of the IMA*, vol. 5, no. 1, pp. 22–75, 2016.
 - [34] A. Beurling, *Collected Works of Arne Buerling: Volume 2, Harmonic Analysis*. Boston, MA: JBirkhäuser, 1989, pp. 351–359.
 - [35] M. Grant and S. Boyd, “CVX: MATLAB software for disciplined convex programming, version 2.1,” Mar. 2014.
 - [36] —, “Graph implementations for nonsmooth convex programs,” in *Recent Advances in Learning and Control*, ser. Lecture Notes in Control and Information Sciences, V. Blondel, S. Boyd, and H. Kimura, Eds. Springer-Verlag Limited, 2008, pp. 95–110.
 - [37] K. C. Toh, M. J. Todd, and R. H. Tütüncü, “SDPT3 - A MATLAB software package for semidefinite programming, version 1.3,” *Optimization Methods and Software*, vol. 11, no. 1–4, pp. 545–581, 1999.